

T. Harvey^{1,2}, W. P. Maksym¹, W. Keel³¹Center for Astrophysics | Harvard and Smithsonian, USA ²University of Southampton, UK ³University of Alabama, USA**Abstract**

Large clouds of ionised gas far from AGN, known as **Extended Emission Line Regions (EELRs)**, promise a novel tool for getting a handle on the kiloyear timescale behavior of AGN accretion. These clouds are often considered as quasar light echoes, because their emission states can encode the AGN luminosity history over the past 100,000 years. AGN with current luminosity below the required luminosity to ionise the EELR are known as **"fading AGN"**. NGC 5972 contains the most extended known EELR and is thought to be a faded AGN, with 2 dex lower luminosity than 5×10^5 years ago (Keel et al. 2017). NGC 5972 is a complex system, so obscuration may also play a role in the variability, along with winds and outflows on different scales.

We present a new analysis of 3 Chandra observations of NGC 5972, totalling 50ks, which take advantage of Chandra's sub-arcsecond angular resolution to analyse spectra, luminosity and potential spatial distribution of hot gas within the galaxy. By comparison to Chandra PSF simulations we determine that the **soft (< 2keV) emission is spatially extended** and show correlation with the HST [OIII] features, including the galaxy-scale EELR and an arcsecond scale nuclear bubble. We also present kinematic analysis of the nuclear bubble based on new Hubble STIS spectra. We are investigating the role of the AGN, jets and possible winds in exciting these features and how **AGN state changes** can contribute to emission patterns.

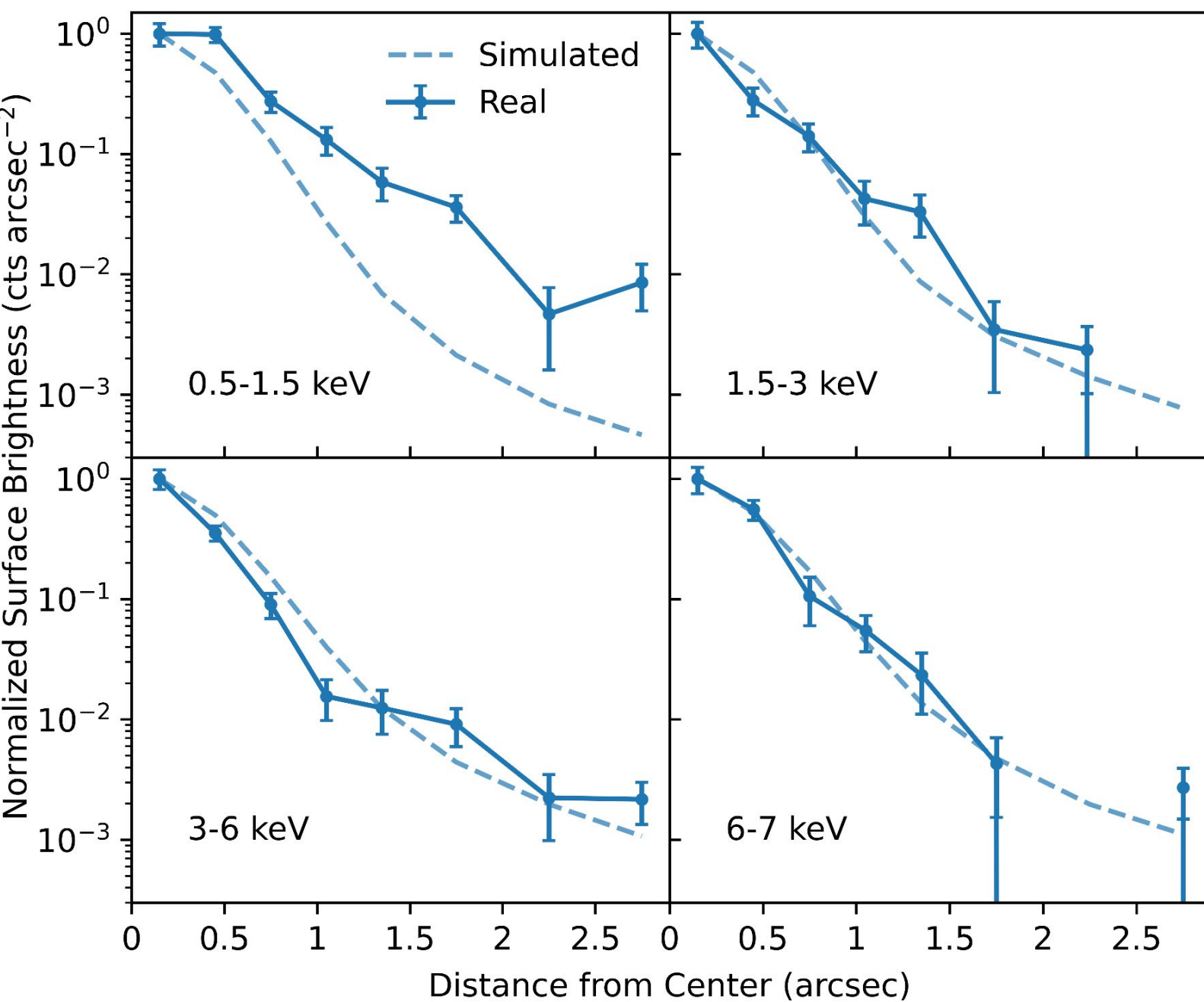


Figure 1 (above) shows the radial surface brightness extracted from concentric annuli around the nucleus for 4 different energy ranges. Different observations are combined and normalised by the counts contained in the central bin. The errors are propagated from Poisson/Gehrels error depending on the number of count. **Figure 2** (below) is similar to Figure 1 but shows the 0.5 - 1.5 keV surface brightness extracted from annuli that have been split into quadrants.

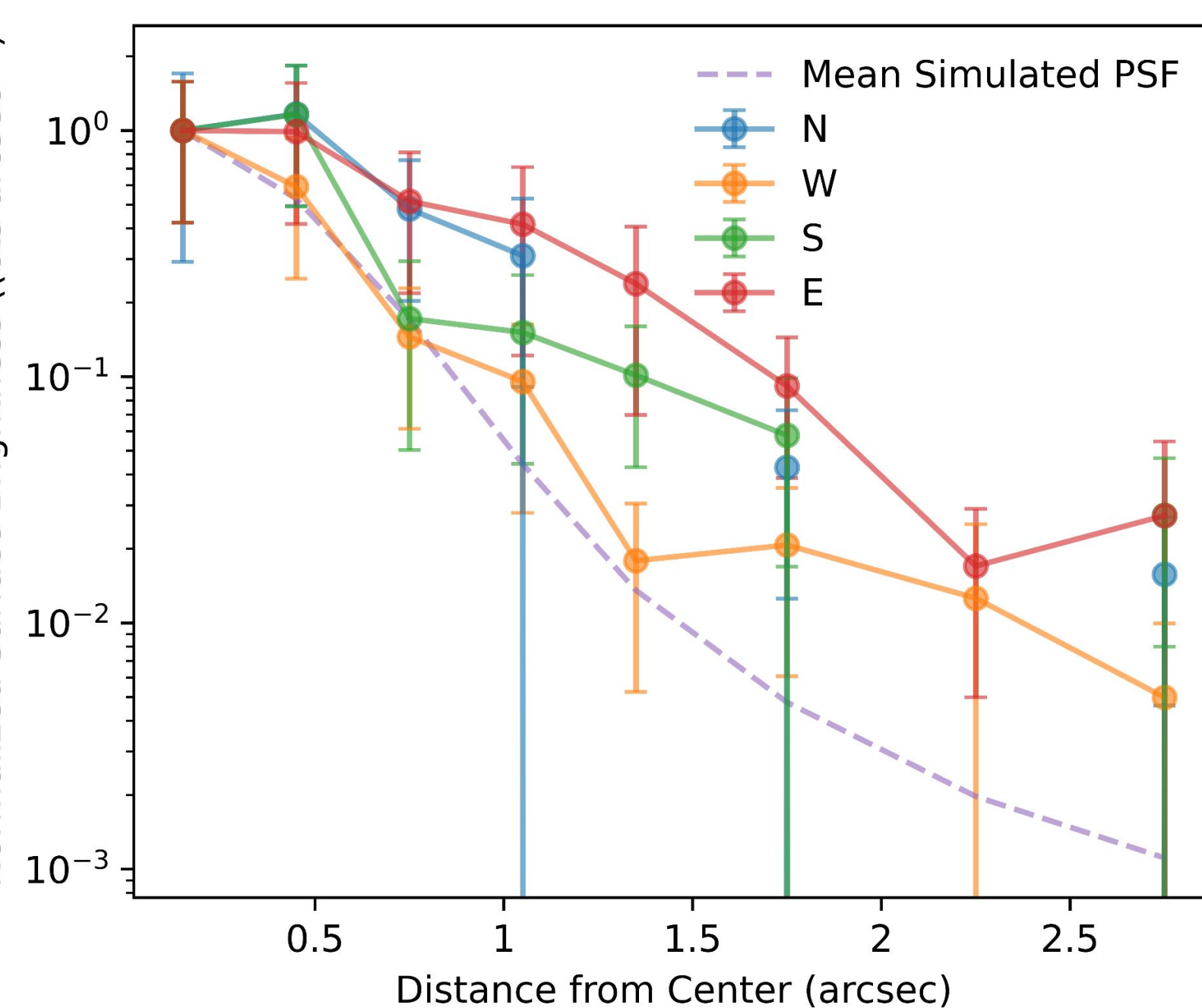


Figure 3 (right) shows the velocity profiles of the H α and [OIII] $\lambda 5007\text{\AA}$ emission lines based on Gaussian fits of the lines and the shift of the best-fit mean relative to the mean value of the line with greatest intensity. Error regions are indicated by shading. **Table 1** (below) contains some computed values for the physical parameters of hot gas within the bubble from APEC fitting.

Parameter	Value
Electron Density (1 st APEC)	$0.24 \pm 0.04 \text{ cm}^{-3}$
Electron Density ([SII])	$430 \pm 250 \text{ cm}^{-3}$
Pressure	$6.1 \pm 1.2 \times 10^{-10} \text{ dyn cm}^{-2}$
Energy Budget	$4.7 \pm 1.3 \times 10^{55} \text{ erg}$
Shock Velocity	$790 \pm 40 \text{ km/s}$
Crossing Time (long axis)	$2.1 \pm 0.2 \text{ Myr}$
Kinetic Luminosity	$8.1 \pm 2.4 \times 10^{41} \text{ erg s}^{-1}$
$L_{\text{kin}}/L_{\text{bol}}$	$1.1 \pm 0.3 \%$
L_{2-10}	$6.17 \times 10^{42} \text{ erg s}^{-1}$
L_{bol}	$7.5_{-1.5}^{+1.3} \times 10^{43} \text{ erg s}^{-1}$

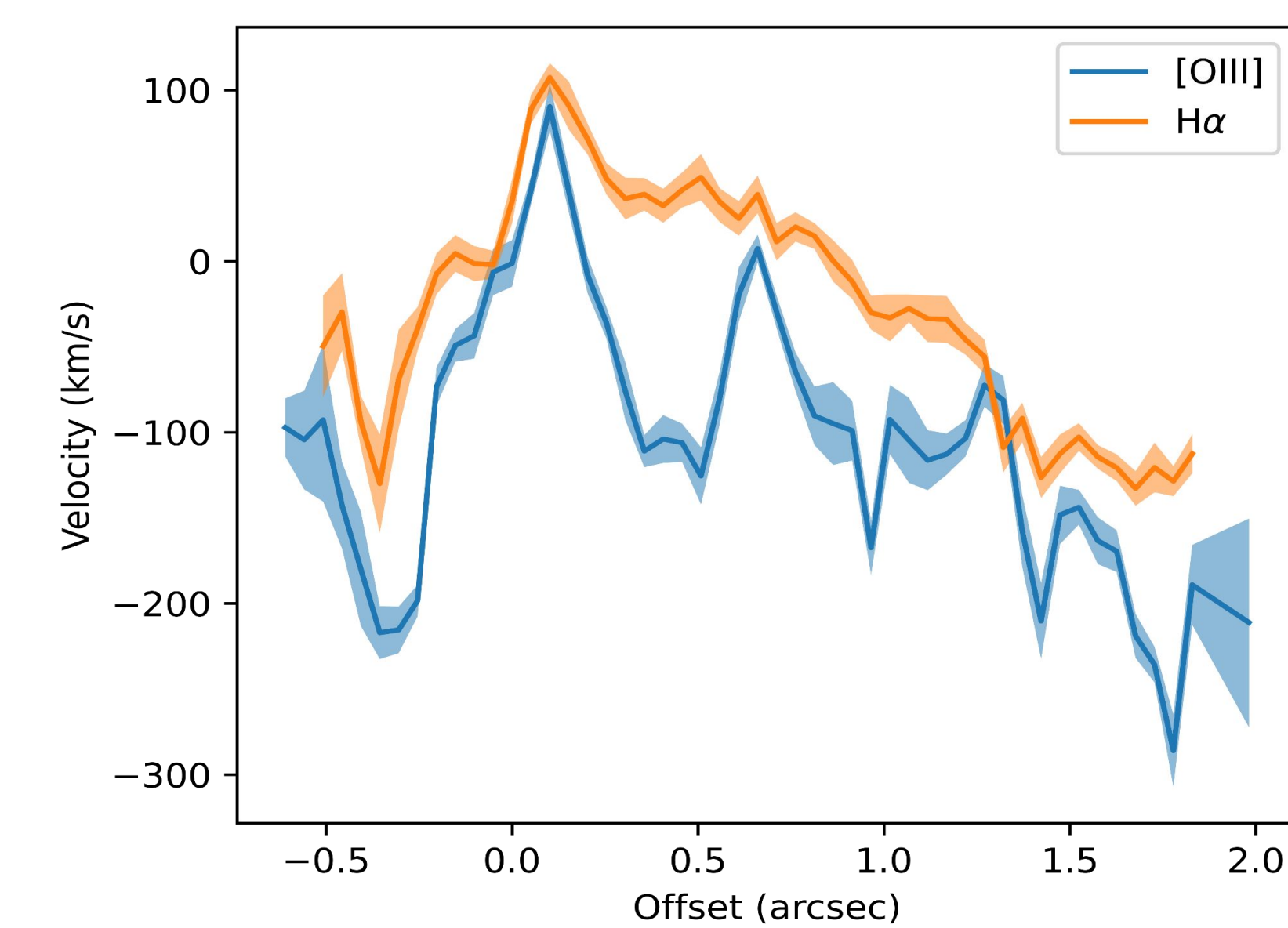


Thomas is researching at the CfA for the final year of his Master's degree. He's looking for observational PhD projects within AGN or galaxy formation and evolution. If you have any questions or would like to discuss this work further, please contact the author.

thomas.harvey@cfa.harvard.edu
www.thomas-harvey.com

Chandra Imaging

- Combined Chandra observations show clear evidence of **co-spatial x-ray emission** in the arm and bubble regions compared to the Hubble [OIII] $\lambda 5007\text{\AA}$ emission. (Image 2)
- Significant soft (0.3-2keV) emission:
 - North Arm: $5.86 \pm 0.85 \times 10^{-15} \text{ erg cm}^{-2} \text{ s}^{-1}$
 - South Arm: $5.05 \pm 0.78 \times 10^{-15} \text{ erg cm}^{-2} \text{ s}^{-1}$
 - Bubble: $2.72 \pm 0.16 \times 10^{-14} \text{ erg cm}^{-2} \text{ s}^{-1}$
- Figure 1** shows results of Chandra PSF modelling to test if the bubble emission is spatially extended:
 - 0.5-1.5 keV emission shows **clear spatial extent** when analysed radially.
 - Soft emission preferentially **extended in the West quadrant**, coincident with the long axis of the [OIII] bubble (Figure 2)
 - Higher energy bands show no significant evidence of extended emission
- Kinematics of gas in bubble analysed using spectral **line fitting of STIS spectra** (G750M, G340L) (Maksym 2015)
 - H α and [OIII] $\lambda 5007\text{\AA}$ line velocities shown in Figure 3 - slit position show in Image 3
 - Velocities generally consistent with the Gemini IFU kinematics
- Our localisation of the AGN within the bubble is complicated by the following
 - 0.2" uncertainty based on *wavdetect* analysis of 6-7 keV FeK α emission.
 - Peak of the [OIII] emission does not match the Chandra AGN location** by $\sim 0.5''$, but does match the continuum peak. X-Ray peak located between [OIII] peaks - see Image 3.
 - Consequences for the kinematic analysis as measured velocities are relative to the strongest [OIII] line.

**Discussion**

The spatial offset between the peak [OIII] emission and nuclear x-ray source gives us clues as to the geometry of the NLR in ways that are suggestive of **selective extinction**, assuming the astrometric match is reliable. The model used in Zhao et al. 2020 constrains the AGN torus/inclination angles (32° , 26°). This suggests the bicone and torus are aligned into the plane of the sky and the [OIII] emission is unexcited (blocked by the torus) or absorbed along our LOS, but we still see NLR FeK α x-rays indicative of reprocessed or shocked emission.

The velocity of the gas from the H α /[OIII] lines is lower than from the x-ray fitting. This could be due to a LOS effect, where the emission line velocity is just the component across the plane of the sky, or it could be a signature of a **multiphase medium**, where the expanding, hot x-ray emitting gas is collimated by a denser, cooler [OIII] shell. This could also explain the density disparity between x-ray and [SII] and the need for a 2nd APEC component in the model.

NGC 5972 shows **misalignment on multiple scales**; on the largest scale the angles of the radio jets and lobes are misaligned to each other and to the EELRs, as is the long axis of the nuclear bubble. The overall misalignment might be explained by the presence of a **double SMBH system**, which could have a more complex system of outflows, jets and ionisation cones. Such double SMBH have been observed, but we commonly observe double-peaked emission lines that are not seen here (Jaiswal et al. 2019). Higher resolution radio observations to better resolve the bubble and jets would provide greater insight into the cause of the misalignment.

The crossing time of the bubble is much longer than the light travel time (about 5 kyr), suggesting the bubble is much **older than the current period of variability** and not related to a recent shock or outflow. The ratio of kinetic to bolometric luminosity is indicative that there is **efficient feedback** that could clear out the gas over large timescales (Hopkins & Elvis 2009), but as L_{bol} has dropped $\sim 100\times$ in the last 5×10^5 yr (Keel et al 2017), this high ratio may not actually indicate meaningful feedback effects. Observations with a proposed mission like Lynx that has better angular resolution and effective area are required to better resolve the full effects of feedback within the bubble.

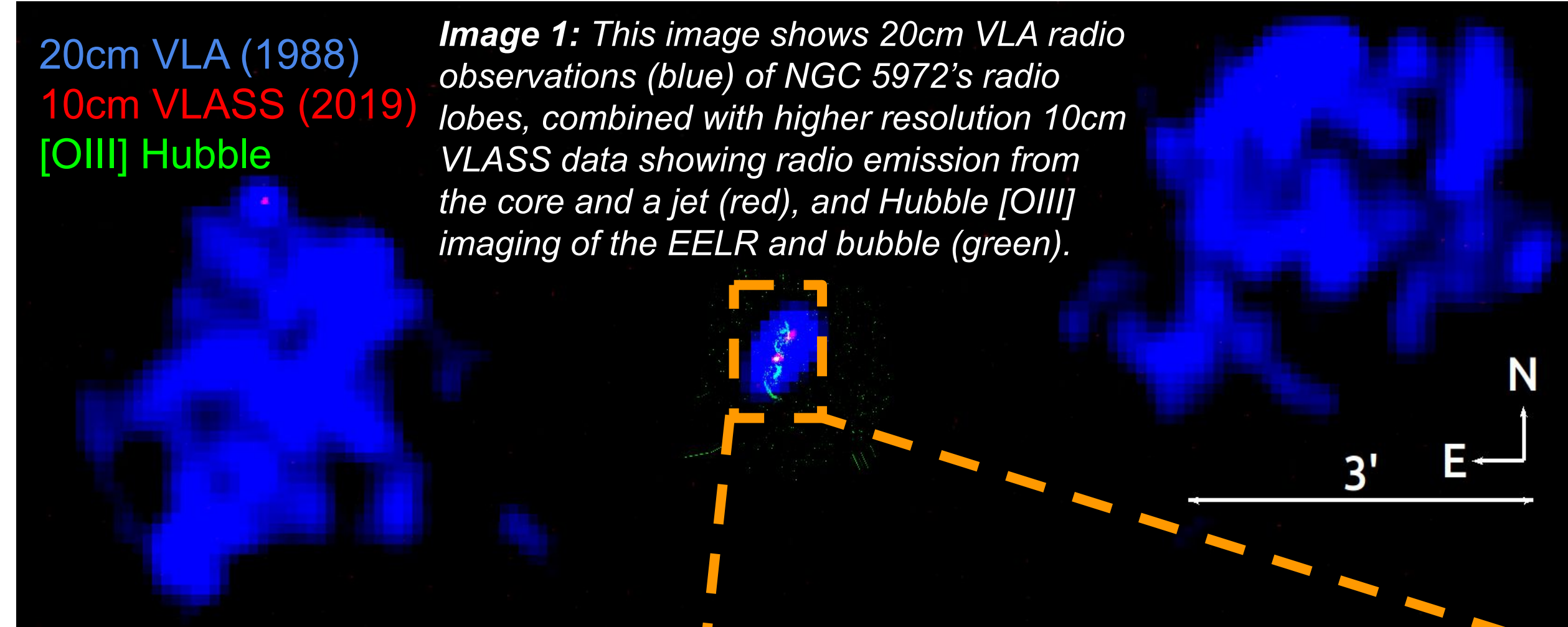


Image 1: This image shows 20cm VLA radio observations (blue) of NGC 5972's radio lobes, combined with higher resolution 10cm VLASS data showing radio emission from the core and a jet (red), and Hubble [OIII] imaging of the EELR and bubble (green).

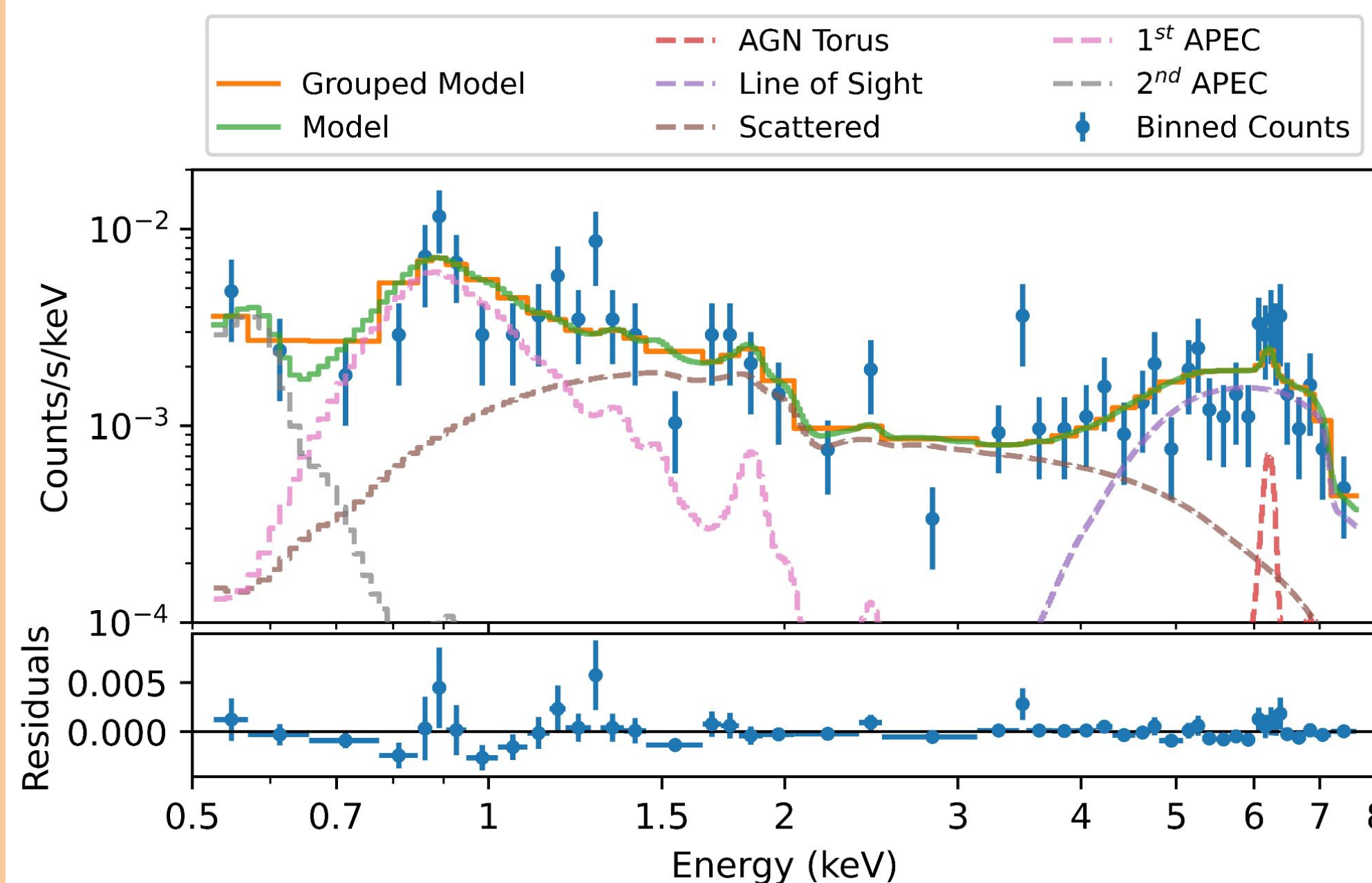


Figure 4 (above) shows the x-ray spectrum of the extracted 2" bubble region shown in Image 2 for the longest observation (obs id 19562). The contribution of different model components are shown with dashed lines. The computed residuals are also shown.

Chandra Spectroscopy

- 0.3-8 keV spectra extracted from 2" region containing nuclear bubble (Figure 4) for each observation
- Fitted to AGN model from Zhao et al (2020), with extra components to model **soft extended emission from hot gas**
- Best fits for these components:
 - Single CLOUDY (Paggi et al. 2012) - RS 0.988
 - $\log N_H = 21.0_{-0.5}^{+0.4}$, $U = 0.59_{-0.07}^{+0.13}$
 - Fitting insensitive to column density.
 - Gas consistent with photo-ionised source.
 - Double APEC (Smith et al. 2001) - RS 1.04
 - 1st: $kT = 0.80 \pm 0.07 \text{ keV}$
 - 2nd: $kT = 0.04 \pm 0.05 \text{ keV}$
 - Gas is consistent with thin collisionally-ionised thermal plasma
- Calculations of physical parameters of the gas due to feedback effects have been calculated from APEC normalisations, shown in Table 1, assuming a **collisional outflow** (detailed in Maksym et al. 2019)
- 2-10 keV X-ray luminosity determined by Zhao et al. 2020 has been used to estimate L_{bol} using correction from Netzer 2019
 - Our L_{bol} greater the FIR estimate (Keel et al. 2012), but consistent with WISE MIR calculation (Keel et al. 2017)
 - Both L_{bol} estimates still ~ 2 dex below upper required ionising luminosity for EELR (Keel et al. 2012).

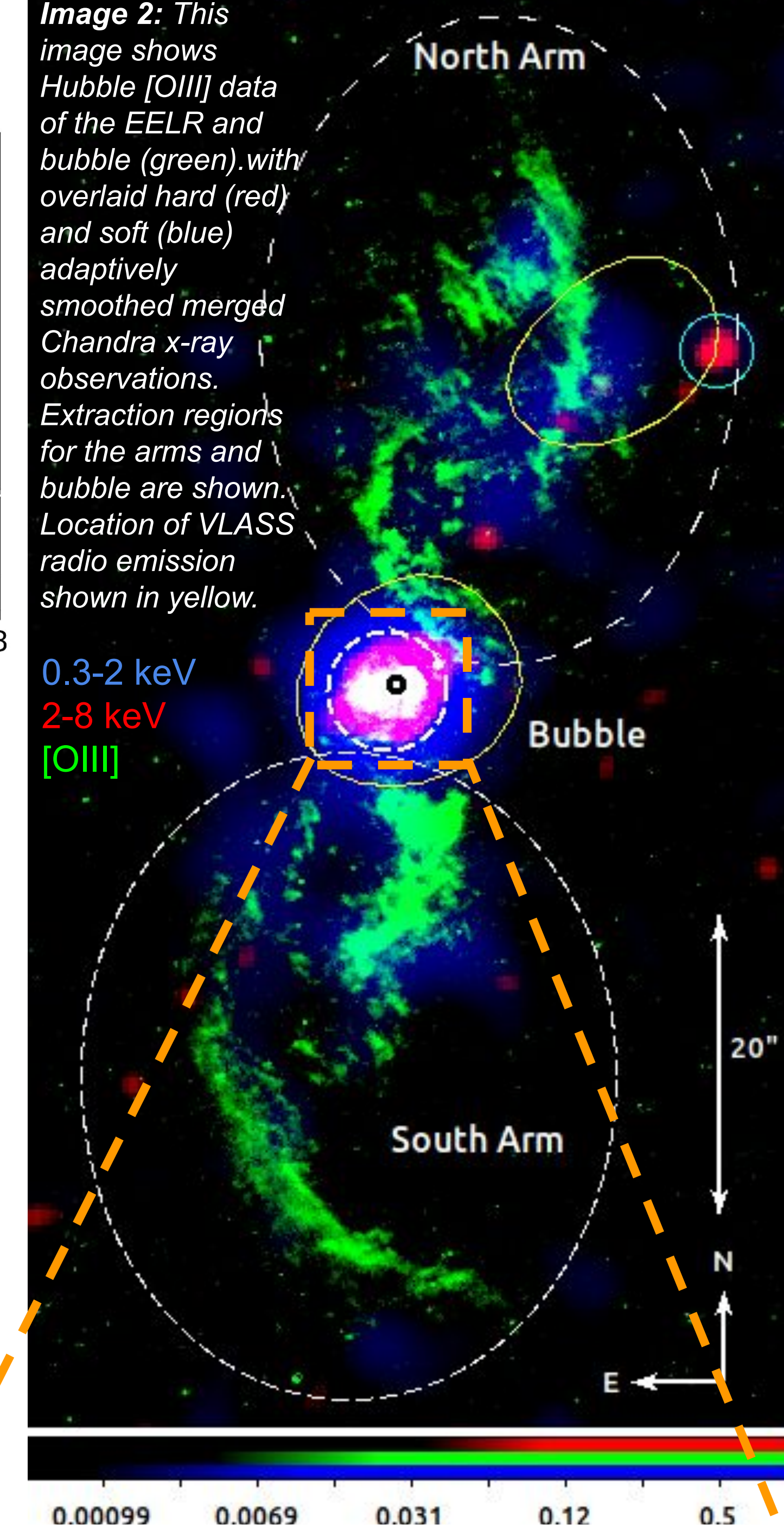


Image 2: This image shows Hubble [OIII] data of the EELR and bubble (green) with overlaid hard (red) and soft (blue) adaptively smoothed merged Chandra x-ray observations. Extraction regions for the arms and bubble are shown. Location of VLASS radio emission shown in yellow.

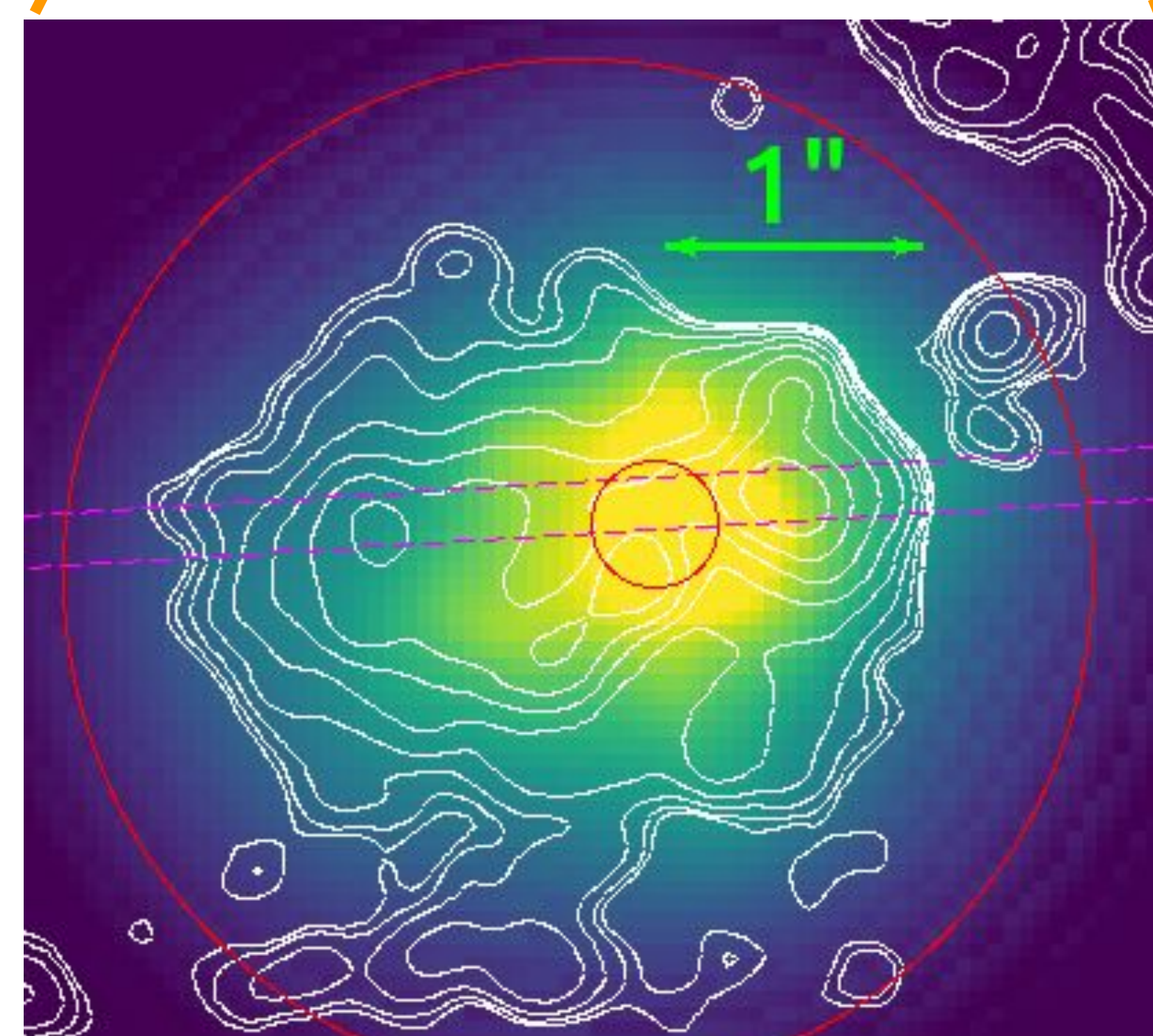


Image 3: shows the adaptively smoothed soft (0.3-2 keV) bubble emission, overlaid with the Hubble [OIII] $\lambda 5007\text{\AA}$ intensity contours. The STIS slit extraction region (purple box), Chandra AGN region (small circle) and the 2" radius bubble region are also shown.

References

- Jaiswal S. et al. (2019), *ApJ* 873. 11.
 Keel W. et al. (2017), *ApJ* 835. : 256.
 Keel W. et al. (2015), *AJ* 149. 155.
 Keel W. et al., (2012), *MNRAS* 420. 878-900
 Maksym W. (2015), *HST Proposal.*: 14271.
 Maksym W. (2016), *CXO Proposal.* 4971.
 Maksym W. et al.,(2019), *ApJ* 872. 94
 Netzer H. (2019), *MNRAS* 488.5185-5191
 Paggi A. et al. (2012), *ApJ* 756. 39.
 Smith R. et al. (2001), *ApJ* 556. L91-L95.
 Zhao X. et al. (2020), *A&A* 650.
 Hopkins P. & Elvis, M. (2009), *MNRAS*, 401(1), 7-14.